Available online at www.sciencedirect.com

ScienceDirect

Current Opinion in Chemical Biology

Molecular simulations of complex carbohydrates and glycoconjugates

Elisa Fadda

Abstract

Complex carbohydrates (glycans) are the most abundant and versatile biopolymers in nature. The broad diversity of biochemical functions that carbohydrates cover is a direct consequence of the variety of 3D architectures they can adopt, displaying branched or linear arrangements, widely ranging in sizes, and with the highest diversity of building blocks of any other natural biopolymer. Despite this unparalleled complexity, a common denominator can be found in the glycans' inherent flexibility, which hinders experimental characterization, but that can be addressed by high-performance computing (HPC)-based molecular simulations. In this short review, I present and discuss the state-of-the-art of molecular simulations of complex carbohydrates and glycoconjugates, highlighting methodological strengths and weaknesses, important insights through emblematic case studies, and suggesting perspectives for future developments.

Addresses

Department of Chemistry and Hamilton Institute, Maynooth University, Ireland

Email address: elisa.fadda@mu.ie (E. Fadda)

Current Opinion in Chemical Biology 2022, **69**:102175

This review comes from a themed issue on **Carbohydrate Bioploymers (2022)**

Edited by **Martina Delbianco** and **Peter H. Seeberger**

For complete overview of the section, please refer to the article collection Carbohydrate Bioploymers (2022)

Available online 18 June 2022

https://doi.org/10.1016/j.cbpa.2022.102175

Introduction

The chemical nature of carbohydrates is deceivingly simple. The general definition of sugars as 'hydrates of carbon" $(CH_2O)_n$ conceals their rich stereochemistry and omits the many diverse groups that can functionalize pyranose and furanose rings through methylation, esterification, deoxygenation, and N-acetylation [1]. For example, N- and O-sulfated sugars are commonly found in glycosaminoglycans (GAGs), with different degrees of sulfation [2-4], potentially regulating and diversifying biological functions [5]. Glycans are built by monosaccharide units connected through glycosidic linkages, which retain non-negligible degrees of freedom in standard conditions of temperature and pressure [6–8]. Furthermore, the associated conformational changes may be accompanied, or triggered by, changes in the ring structure [9–13], also known as pucker [14,15], see Figure 1. This 'intrinsic disorder', to draw a parallel with proteins, determines that the 3D equilibrium structures of glycans should be described more appropriately by weighted conformational ensembles rather than by single conformers. This remarkable architectural feature also renders glycans partially or completely invisible to structural biology techniques.

Glycosidic linkages are defined by the values of the φ (O5C1O1Cx) and ψ (C1O1CxCx-1) torsion angles for 1/2-(2,3,4) linkages, with the addition of the ω (C1O1C6C5) torsion angle values for 1/2–6 linkages [16], see Figure 2. The rotational degrees of freedom around glycosidic linkages are remarkably restrained to specific conformations dictated by stereoelectronic effects [6]. More specifically, for two linked pyranoses in $^4C_1$ chair conformation, see Figure 1, the exoanomeric effect [17] determines that the φ torsion is found preferentially in a ± *gauche* conformation relative to the O5 ring oxygen (φ = ± 70°), while the ψ torsion will adopt value(s) corresponding to a minimum steric compression, usually around ψ = 180° in disaccharides [18]. In 1/2–6 linkages, the ω torsion can populate two or three different energy basins at ω = ± 60° and 180°. The relative populations of the resulting rotamers in 1/2–6 linkages can change dramatically in response to a 'gauche effect' between the O6 and the neighboring O5 ring oxygen, or the O4, which can be axial in galactopyranoses, or equatorial in gluco/mannopyranoses [6], and to steric compression and/or intramolecular interactions in large, branched glycans [19–21]. Ultimately, the high conformational flexibility of glycans derives from the existence of different preferred rotameric states and from the rotational degrees of freedom associated with those states at room temperature, estimated to range up to 15°–20° for each torsion [6,19,20]. As a result, the longer and more branched the glycan is, the higher the inherent dynamics of its structure, further enhanced when it contains 1/2–6 linkages. More to this in the section below.

Figure 1

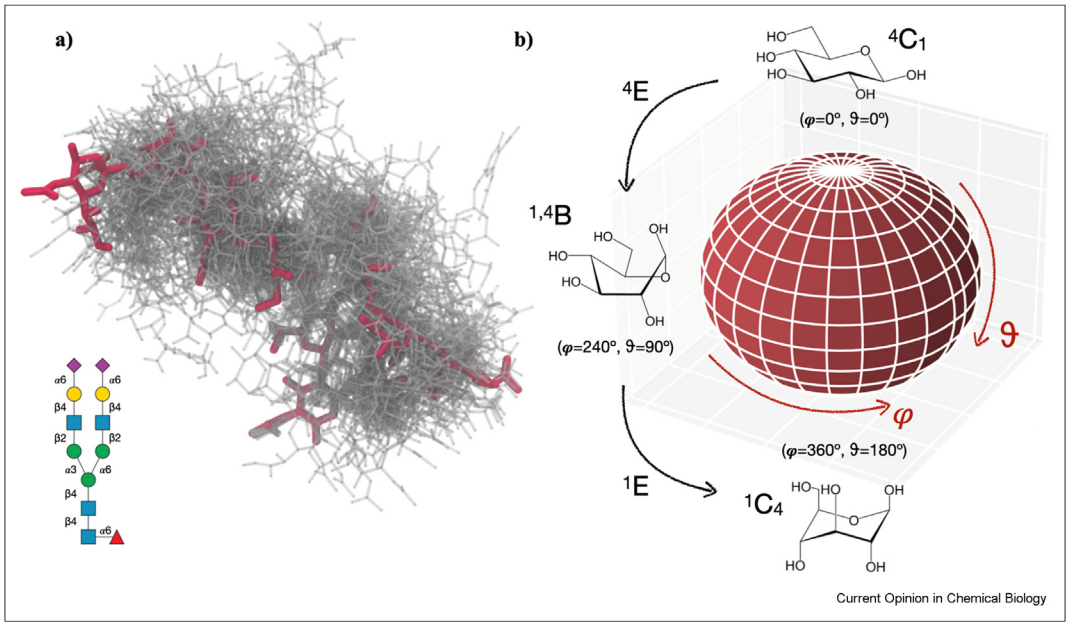

Panel (a) Graphical representation of the conformational ensemble of the FA2G2S2 (mammalian) N-glycan from Ref. [19], shown with the 2D SNFG notation [22,23] on the bottom-left corner. Snapshots from the MD simulation (collected every 50 frames over a 500 ns trajectory) are shown with grey sticks, with a structure representative of the highest populated cluster shown with thicker red sticks. **Panel (b)** 2D structures, symbols, and arrows highlighting one of the pseudorotational paths accessible to the glucopyranose ring [9] connecting the two chair conformations at the poles, based on the Cremer–Pople puckering coordinates [14]. The longitude and latitude lines on the spheroid represent potential conformational itineraries. Molecular rendering with *vmd* (https://www.ks.uiuc.edu/Research/vmd/), 3D plot of spherical coordinates rendered with *seaborn* (https://seaborn.pydata.org), 2D glycan structure representation rendered with *DrawGlycan-SNFG* [24] (http://www.virtualglycome.org/DrawGlycan/).

Computational methods for 3D structure determination of glycans and glycoconjugates

The relative conformational preference of complex carbohydrates at equilibrium in standard conditions depends not only on the electronic structure considerations discussed above, but is also modulated by the environment, and by intra and intermolecular contacts. This scenario can rapidly lead to a degree of complexity [25] that is difficult, if not impossible, to represent accurately with the means dictated by the current technology. The nature of the molecular insight we seek through simulations and the size of the system at hand are the main determinants in the choice of computational approach, ranging from a full description of the electronic structure through quantum mechanical (QM)-based approximations, to much less computationally demanding classical representations through all-atom empirical force fields (MM), commonly explored through Newtonian molecular dynamics (MD). Coarse-grained representations are not discussed here, and on this subject, the reader is referred to a recent comprehensive review [26].

QM is essential for the prediction of spectroscopic properties of carbohydrates and for calculating reaction coordinates with corresponding energy profiles [27]. The latter hinges on the unique ability of fully electronic representations to accurately describe the conformational transitions that the sugar ring undergoes along specific reaction coordinates, a point that is especially relevant to enzymatic catalysis [28–30]. Within the context of studies of the binding specificity and catalytic activity of carbohydrate-active enzymes (CAZymes), the electronic structure information obtained by first-principle (*ab initio*) methods can be complemented by a classical description of the surrounding protein environment through QM/MM hybrid approaches within a static or a dynamic framework [27,31,32]. QM/MD approaches allow us to explore reaction profiles in standard thermodynamic conditions within a dynamic protein environment. As a recent and notable application of this technique, Nin-Hill and Rovira used classical MD combined with QM/MM metadynamics [33–35] to define the reaction mechanism of β-galactocerebrosidase, a glycoside hydrolase essential for the catabolism of glycosphingolipids, found to be mutated in Krabbe disease [36].

Molecular simulations can also be used to obtain atomistic insight on the recognition of glycan moieties by glycan-binding proteins (lectins) and to understand the effects of glycosylation on protein structure and function. To address these (very computationally expensive)

Figure 2

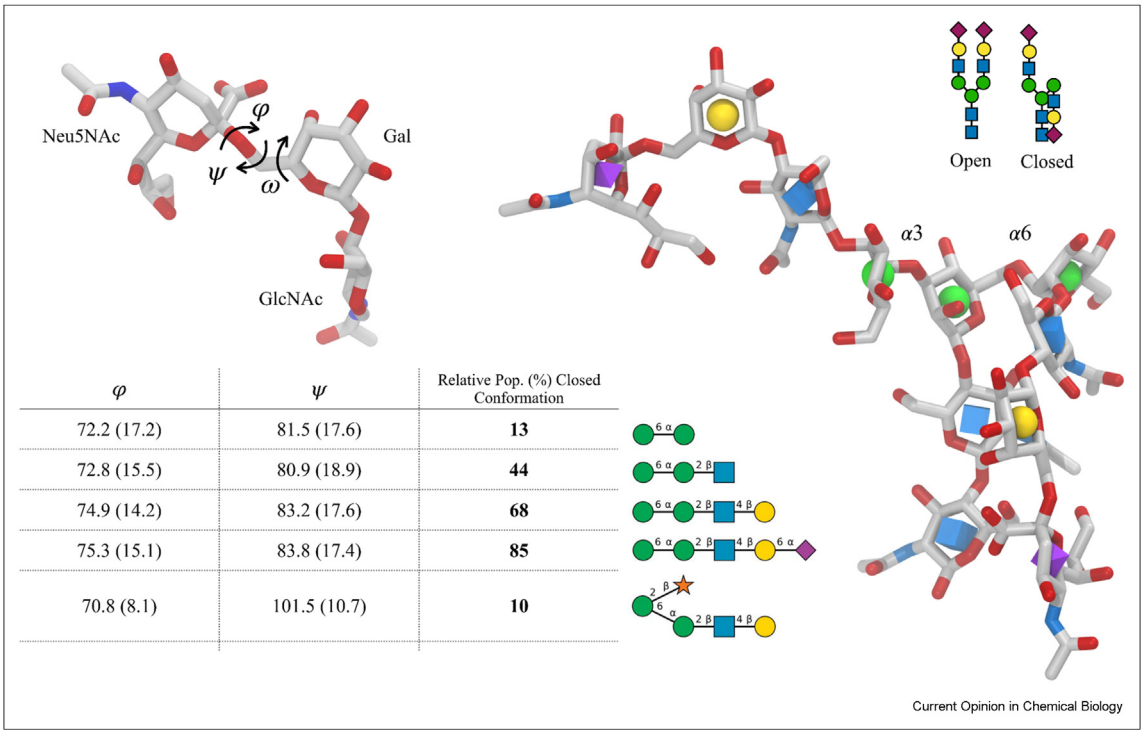

φ	ψ	Relative Pop. (%) Closed Conformation
72.2 (17.2)	81.5 (17.6)	**13**
72.8 (15.5)	80.9 (18.9)	**44**
74.9 (14.2)	83.2 (17.6)	**68**
75.3 (15.1)	83.8 (17.4)	**85**
70.8 (8.1)	101.5 (10.7)	**10**

A representative 3D conformation of the Neu5NAc-α(2−6)-Gal-β(1−4)-GlcNAc (or sLacNAc) epitope is shown on the top-left side, with the φ, ψ, and ω torsion angles defining the α(2−6) linkage indicated. On the right-hand side, the 3D atomistic structure of a 'closed' conformation of a complex biantennary N-glycan (A2G2S2), with an SNFG 2D sketch of the 'open' and 'closed' conformations on the top-right corner. The table shows the equilibrium values of the φ and ψ torsion angles corresponding to the 'closed' conformation of the Man-α(1−6)-Man linkage in biantennary complex N-glycans, with changes in relative populations in function of sequence [19,21]. The ω torsion angle values do not affect the open/closed equilibrium of the α(1−6) arm and can be retrieved from the original publications. Symbols correspond to the SNFG nomenclature [22,23]. Molecular rendering with *vmd* (https://www.ks.uiuc.edu/Research/vmd/), 2D glycan structure representation rendered with *DrawGlycan-SNFG* [24] (http://www.virtualglycome.org/DrawGlycan/).

questions, conformational sampling based on classical mechanics should be used to retrieve the weighted ensembles that define the glycans 3D structure at equilibrium. Within an MM approximation, the stereoelectronic effects controlling the conformation of glycosidic linkages, together with the ring pucker preferences, are 'hard coded' into empirical force field parameters [6,37,38]. The most widely used and developed all-atoms additive force fields for carbohydrates to date are GLYCAM06 [39−41] and CHARMM36 [42−46], with parameters available for most pyranoses and furanoses in eukaryotic, prokaryotic, and viral glycans [47−49]. The full complementarity of these force fields to the AMBER and CHARMM families of parameter sets, respectively, allows for the accurate representation of complex glycoconjugates [37,38,42] featuring both structured and disordered protein regions [50,51], where glycosylation can affect the protein's conformation, both locally and globally [52−55]. Other empirical parameter sets include the united atoms representation in GROMOS [18,56-59] and the all-atoms representation in OPLS-AA [60,61]. These force fields cover a narrower selection of monosaccharides and linkages and are suitable for the simulation of unlinked glycans.

The parameterization of all empirical additive force fields for carbohydrates follows the principles and protocols used in the development of the 'parent' protein force field to ensure complementarity [38,62]. As a limitation of the model, additive protein force fields are known to overestimate protein−protein interactions relative to protein-water interactions [63−65], whicht can lead to an unbalanced representation of structure versus disorder, and to enhanced protein compactness and non-physical aggregation [63,66−68]. While maintaining the balance of the additive force field parameter set, these effects can be mitigated by scaling Lennard−Jones (LJ) parameters [65,66,69,70], as one of the most common strategies used to weaken protein−protein contacts or to strengthen protein-water interactions, or even to strengthen water−water interactions as an indirect approach [71].

It may not be surprising to realize that additive force fields for carbohydrates suffer from a similar imbalance,

favoring carbohydrate−carbohydrate/protein interactions relative to carbohydrate−water interactions. These effects are principally due to the overpolarization of the hydroxyl groups in the gasphase, which is necessary to obtain a correct representation of the structure and energy of the systems in an aqueous environment. The resulting increased electrostatic attraction between hydroxyl groups has been shown to lead to the underestimation of the ΔH_{vap} of glycerol [68], the collapse of specific L-Rha polysaccharide chains [72], artificial aggregation [73,74] and is most likely the cause of the overtwisting of cellulose fibrils [75]. For simulations with GLYCAM06, rescaling of LJ parameters [75], as well as the use of the TIP5P water model [76,77] with diffusion properties closer to experiment, instead of the TIP3P model used in its parameterization [39], can alleviate or even eliminate these issues [74,75,78]. As a note of caution standing in all cases of mixed force fields approaches [63,79], the benefits of using a different water model can be due to a cancellation of errors, and thus, the effects may not be necessarily generalizable. The better behavior of CHARMM36 in this context may be reconciled with a lower solute−solute interaction strength resulting from the original parameterization [72,73], yet both GLYCAM06 and CHARMM36 representations have been found to benefit from scaling of the LJ ε values to reproduce experimental osmotic coefficients [73]. The use of polarizable (or non-additive) force fields is a more coherent solution to these shortcomings [68]; more to this in the Conclusions and Perspectives section.

Insight into the 3D structure of glycans and glycoproteins from molecular simulations

Despite the simplicity of the MM formalism and the limitations of the additive electrostatic charges scheme, empirical force fields have been shown to be remarkably successful at representing the structure and dynamics of glycans and glycoconjugates. Indeed, classical MD simulations can be highly informative when accompanied by sufficient sampling, necessary to retrieve all the 3D structures representative of the conformational ensemble with corresponding weights [80]. As discussed earlier, the conformational propensity of the glycosidic linkages is restricted to specific energy basins, with flexibility determined by their relative accessibility and by the inherent degrees of freedom around the φ, ψ, and ω torsions, see Figure 2. This information can be retrieved successfully through classical MD simulations, where the structure of short and conformationally restrained glycans can be obtained as a combination of accessible disaccharide blocks, as shown by Turupcu and Oostenbrink through free energy calculations [81].

As the glycans' structure grows in terms of length and branching, and especially when it includes highly flexible 1/2−6 linkages, the relative populations of the rotamers change dramatically with sequence [19,20]. Extensive sampling through classical MD showed that the conformation of the (1−6) arm in complex biantennary N-glycans undergoes a transition between 'open' and 'closed' states at equilibrium, see Figure 2. In the open conformation, the (1−6) arm is exposed to the solvent and thus, easily accessible to CAZymes, while in the closed conformation, the (1−6) arm folds over the GlcNAc-β(1−4)-GlcNAc core, see Figure 2, likely hindering functionalization. As summarized, in the table, in Figure 2 and discussed in Refs. [19,21], upon galactosylation, the (1−6) arm becomes predominantly closed, which provides a rationale to explain why the (1−6) arm in complex N-glycans is more difficult to functionalize than the (1−3) arm, which remains exposed [19]. Within this framework, further insight from MD simulations shows that the addition of β(1−2)-linked Xyl to the central Man reverses the open/closed equilibrium [21], providing a strategy for the selective functionalization of the arms for synthetic applications. Also, the presence of a bisecting GlcNAc has been shown by replica exchange MD (REMD) to affect conformation in shorter N-glycans [82,83].

When glycans are linked to glycoproteins, MD simulations have shown that the interaction with the protein surface can shift the conformational equilibrium of the glycan, favoring structures that complement the surrounding protein landscape. Emblematic in this case is the recognition of a very low populated 'open' conformation of the Lewis X epitope [80] by the *Ralstonia solanacearum* lectin [84], where interactions with the protein surface compensate for the high energy cost of shifting the conformational equilibrium. Interactions with the protein surface can also limit the accessibility of selected (or all) branches (arms) of oligomannose N-glycans [20] and thus can modulate the type of glycosylation at specific sites [20,85], as well as glycan recognition.

Classical MD simulations have also revealed some of the many roles of glycans in the structure, stability, dynamics, and function of glycoproteins [52,85−88], and more recently, provided crucial insight into the role of glycosylation in viral infection [89−112]. Notable among these many contributions, is the work of the Amaro lab and colleagues [91,92] in revealing, for the first time, in a viral fusion protein, the functional role of the glycan shield in the activation mechanism of the SARS-CoV-2 spike (S), see Figure 3. Also, work from Harbison et al. [110] indicated that the nature and topology of the glycan shield can modulate the S glycoprotein's activity and that the evolution of the shield represents a strategy to enhance viral infectivity, see Figure 3, as recently supported by experimental evidence [113,114].

Conclusions and perspectives

Technological advances in HPC and in distributed computing provided in recent years the means to show

Figure 3

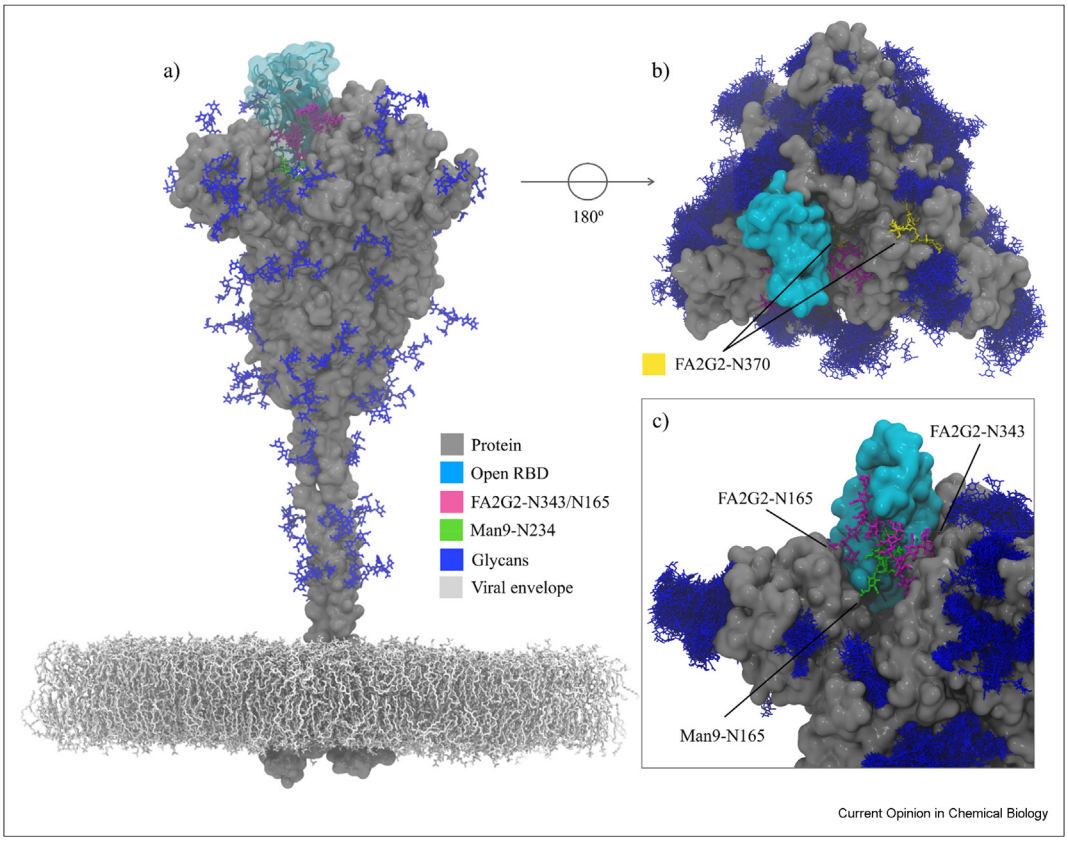

Panel a) Atomistic model of the fully glycosylated SARS-CoV-2 (Wuhan-Hu-1) spike (S) glycoprotein with the receptor-binding domain (RBD) of chain A in an open conformation from Ref. [91]. Colour coding is indicated in the legend. **Panel b)** Top view of the SARS-CoV-2 S A372T glycoprotein from Ref. [110], showing the FA2G2-N370 glycan, recently lost along the SARS-CoV phylogeny, binding a cleft on the closed RBD of chain B and filling the pocket left vacant by the opening of the RBD of chain A (cyan). **Panel c)** Close up of the cleft left vacant by the opening on the SARS-CoV-2 S RBD of chain A and filled by the Man9-N234 glycan (green). The two FA2G2 N-glycans at N343 and N165 (purple) are shown supporting the RBD open conformation [91,92,110]. Molecular rendering with *vmd* (https://www.ks.uiuc.edu/Research/vmd/).

the true potential of molecular simulations for the study of the structure and function of complex biomolecules. This is especially true in the case of simulations of complex carbohydrates and glycoconjugates, historically left to the sidebench due to the inherent structural and chemical complexity of glycans and their not-always-obvious presence and contribution to biomolecular function, and now attracting more attention as a consequence of the drive for scientific advances in response to the COVID-19 pandemic.

In this review, I have shown a few recent examples of how molecular simulations within QM, MM, and hybrid schemes have successfully addressed important questions on the role of carbohydrates in health and disease. Yet, big challenges remain in terms of computing infrastructure, which limits sampling within a fully electronic description, and in terms of limitations of the MM additive force field formalism, which can produce non-physical outcomes even in the context of exhaustive sampling. Pioneering work from the Mackerell's lab shows that the introduction of charge polarizability based on the classical Drude oscillator model solves many of the problems resulting from the description of carbohydrates by additive force fields [62,68,115-118]. Drude simulations are twice as computationally expensive as conventional MD simulations with non-polarizable force fields [62,119], which may be problematic when dealing with large biomolecular systems, but worth the investment in the case of simulations of heterogeneous, dense, and dynamic environments, such as bacterial biofilms or extracellular matrix models.

Machine learning force fields [120] represent a game-changing methodological development that would allow us to perform exhaustive simulations of increasingly large systems within realistically complex environments by narrowing the gap between QM accuracy and MM computational efficiency. Notable examples in this context are the ANI-1 potential [121]

with an excellent performance against DFT references, TensorMol [122] reproducing vibrational spectra of small organic molecules with DFT accuracy, and also able to run proof-of-concept neural network MD simulations of small proteins, and more recently TorchMD-Net [123] molecular potentials, achieving the most accurate predictions of QM properties to date. These advances are an exciting prospect for a step change also in glycoscience discovery through computing, while we can also look forward to HPC technology revolutions, such as the introduction of quantum computing, that will provide unprecedented algorithmic speed-ups [124-127].

Declaration of competing interest

The authors declare that they have no known competing financial interests or personal relationships that could have appeared to influence the work reported in this paper.

Acknowledgements

This work was supported by the Science Foundation of Ireland (20/FFP-P/8809). The opinions, findings, and conclusions or recommendations expressed in this material are those of the author(s) and do not necessarily reflect the views of the Science Foundation Ireland.

References

Papers of particular interest, published within the period of review, have been highlighted as:

* of special interest
** of outstanding interest

1. Seeberger PH: **Monosaccharide diversity**. In *Essentials of glycobiology*. Edited by Varki A, Cummings RD, Esko JD, Stanley P, Hart GW, Aebi M, Darvill AG, Kinoshita T, Packer NH, Prestegard JH, *et al.*, Cold Spring Harbor Laboratory Press; 2017.

2. Song Y, Zhang F, Linhardt RJ: **Analysis of the glycosaminoglycan chains of proteoglycans**. *J Histochem Cytochem* 2021, **69**:121–135.

3. Fu L, Suflita M, Linhardt RJ: **Bioengineered heparins and heparan sulfates**. *Adv Drug Deliv Rev* 2016, **97**:237–249.

4. Chen Y-H, Narimatsu Y, Clausen TM, Gomes C, Karlsson R, Steentoft C, Spliid CB, Gustavsson T, Salanti A, Persson A, *et al.*: **The GAGOme: a cell-based library of displayed glycosaminoglycans**. *Nat Methods* 2018, **15**:881–888.

5. Gama CI, Tully SE, Sotogaku N, Clark PM, Rawat M, Vaidehi N, Goddard 3rd WA, Nishi A, Hsieh-Wilson LC: **Sulfation patterns of glycosaminoglycans encode molecular recognition and activity**. *Nat Chem Biol* 2006, **2**:467–473.

6. ** Woods RJ: **Predicting the structures of glycans, glycoproteins, and their complexes**. *Chem Rev* 2018, **118**:8005–8024.
Excellent recent review on the strengths and limitations of empirical additive force fields for the simulations of complex carbohydrates

7. Poveda A, Fittolani G, Seeberger PH, Delbianco M, Jiménez-Barbero J: **The flexibility of oligosaccharides unveiled through residual dipolar coupling analysis**. *Front Mol Biosci* 2021, **8**:784318.

8. Yang M, MacKerell Jr AD: **Conformational sampling of oligosaccharides using Hamiltonian replica exchange with two-dimensional dihedral biasing potentials and the weighted histogram analysis method (WHAM)**. *J Chem Theor Comput* 2015, **11**:788–799.

9. Mayes HB, Broadbelt LJ, Beckham GT: **How sugars pucker: electronic structure calculations map the kinetic landscape of five biologically paramount monosaccharides and their implications for enzymatic catalysis**. *J Am Chem Soc* 2014, **136**:1008–1022.

10. García-Herrero A, Montero E, Muñoz JL, Espinosa JF, Vián A, García JL, Asensio JL, Javier Cañada F, Jiménez-Barbero J: **Conformational selection of glycomimetics at enzyme catalytic sites: experimental demonstration of the binding of distinct high-energy distorted conformations of C-, S-, and O-glycosides by E. Coli β-galactosidases**. *J Am Chem Soc* 2002, **124**:4804–4810.

11. Alibay I, Bryce RA: **Ring puckering landscapes of glycosaminoglycan-related monosaccharides from molecular dynamics simulations**. *J Chem Inf Model* 2019, **59**:4729–4741.

12. Muñoz-García JC, Corzana F, de Paz JL, Angulo J, Nieto PM: **Conformations of the iduronate ring in short heparin fragments described by time-averaged distance restrained molecular dynamics**. *Glycobiology* 2013, **23**:1220–1229.

13. Kato K, Yamaguchi T: **Paramagnetic NMR probes for characterization of the dynamic conformations and interactions of oligosaccharides**. *Glycoconj J* 2015, **32**:505–513.

14. Cremer D, Pople JA: **General definition of ring puckering coordinates**. *J Am Chem Soc* 1975, **97**:1354–1358.

15. Jeffrey GA, Yates JH: **Stereographic representation of the cremer-pople ring-puckering parameters for pyranoid rings**. *Carbohydr Res* 1979, **74**:319–322.

16. Wormald MR, Petrescu AJ, Pao Y-L, Glithero A, Elliott T, Dwek RA: **Conformational studies of oligosaccharides and glycopeptides: complementarity of NMR, X-ray crystallography, and molecular modelling**. *Chem Rev* 2002, **102**:371–386.

17. Tvaroška I, Bleha T: **Anomeric and exo-anomeric effects in carbohydrate chemistry**. In *Advances in carbohydrate chemistry and biochemistry*. Edited by Tipson RS, Horton D, Academic Press; 1989:45–123.

18. Perić-Hassler L, Hansen HS, Baron R, Hünenberger PH: **Conformational properties of glucose-based disaccharides investigated using molecular dynamics simulations with local elevation umbrella sampling**. *Carbohydr Res* 2010, **345**:1781–1801.

19. ** Harbison AM, Brosnan LP, Fenlon K, Fadda E: **Sequence-to-structure dependence of isolated IgG Fc complex biantennary N-glycans: a molecular dynamics study**. *Glycobiology* 2019, **29**:94–103.
Extensive sampling through conventional (parallel) MD simulations shows that the equilibrium conformation and dynamics of biantennary complex N-glycans depend on their sequence.

20. * Fogarty CA, Fadda E: **Oligomannose N-glycans 3D architecture and its response to the FcγRIIIa structural landscape**. *J Phys Chem B* 2021, **125**:2607–2616.
Extensive sampling through parallel conventional MD simulations determines the sequence/branching-to-structure relationship in oligomannose N-glycans, with important insight on how the protein landscape can shift the conformational equilibrium, ultimately modulating glycan biosynthesis.

21. * Fogarty CA, Harbison AM, Dugdale AR, Fadda E: **How and why plants and human N-glycans are different: insight from molecular dynamics into the "glycoblocks" architecture of complex carbohydrates**. *Beilstein J Org Chem* 2020, **16**:2046–2056.
Extensive sampling through parallel conventional MD simulations provides further insight into the dependence of N-glycans' structure on sequence and branching, with a perspective on a bottom-up approximation for the reconstruction of complex N-glycans through 'glycoblocks.'

22. Varki A, Cummings RD, Aebi M, Packer NH, Seeberger PH, Esko JD, Stanley P, Hart G, Darvill A, Kinoshita T, *et al.*: **Symbol nomenclature for graphical representations of glycans**. *Glycobiology* 2015, **25**:1323–1324.

23. Neelamegham S, Aoki-Kinoshita K, Bolton E, Frank M, Lisacek F, Lütteke T, O'Boyle N, Packer NH, Stanley P, Toukach P, *et al.*:

Updates to the symbol nomenclature for glycans guidelines. *Glycobiology* 2019, **29**:620–624.

24. Cheng K, Zhou Y, Neelamegham S: **DrawGlycan-SNFG: a robust tool to render glycans and glycopeptides with fragmentation information**. *Glycobiology* 2017, **27**:200–205.

25. Noda N, Jung Y, Ado G, Mizuhata Y, Higuchi M, Ogawa T, Ishidate F, Sato S-I, Kurata H, Tokitoh N, *et al.*: **Glucose as a protein-condensing cellular solute**. *ACS Chem Biol* 2022, https://doi.org/10.1021/acschembio.1c00849.

26. * Perez S, Fadda E, Makshakova O: **Computational modeling in glycoscience**. *Comprehensive Glycoscience* 2021, https://doi.org/10.1016/b978-0-12-819475-1.00004-3.
Overview of computational methods and approximations from QM to coarse-graining with applications in computational glycoscience.

27. * Ardèvol A, Rovira C: **Reaction mechanisms in carbohydrate-active enzymes: glycoside hydrolases and glycosyltransferases. Insights from ab initio quantum mechanics/molecular mechanics dynamic simulations**. *J Am Chem Soc* 2015, **137**:7528–7547.
Review and perspective on the insight provided by QM and hybrid computational schemes on CAZymes' catalysis.

28. Biarnés X, Nieto J, Planas A, Rovira C: **Substrate distortion in the michaelis complex of Bacillus 1,3–1,4-β-Glucanase: insight from first principles molecular dynamics simulations ***. *J Biol Chem* 2006, **281**:1432–1441.

29. Thompson AJ, Dabin J, Iglesias-Fernández J, Ardèvol A, Dinev Z, Williams SJ, Bande O, Siriwardena A, Moreland C, Hu T-C, *et al.*: **The reaction coordinate of a bacterial GH47 α-mannosidase: a combined quantum mechanical and structural approach**. *Angew Chem Int Ed Engl* 2012, **51**:10997–11001.

30. Morais MAB, Coines J, Domingues MN, Pirolla RAS, Tonoli CCC, Santos CR, Correa JBL, Gozzo FC, Rovira C, Murakami MT: **Two distinct catalytic pathways for GH43 xylanolytic enzymes unveiled by X-ray and QM/MM simulations**. *Nat Commun* 2021, **12**:1–13.

31. Brunk E, Rothlisberger U: **Mixed quantum mechanical/molecular mechanical molecular dynamics simulations of biological systems in ground and electronically excited states**. *Chem Rev* 2015, **115**:6217–6263.

32. Mendoza F, Masgrau L: **Computational modeling of carbohydrate processing enzymes reactions**. *Curr Opin Chem Biol* 2021, **61**:203–213.

33. Barducci A, Bonomi M, Parrinello M: **Metadynamics**. *Wiley Interdiscip Rev Comput Mol Sci* 2011, **1**:826–843.

34. Bussi G, Laio A: **Using metadynamics to explore complex free-energy landscapes**. *Nature Reviews Physics* 2020, **2**:200–212.

35. Raich L, Nin-Hill A, Ardèvol A, Rovira C: **Enzymatic cleavage of glycosidic bonds: strategies on how to set up and control a QM/MM metadynamics simulation**. *Methods Enzymol* 2016, **577**:159–183.

36. ** Nin-Hill A, Rovira C: **The catalytic reaction mechanism of the β-galactocerebrosidase enzyme deficient in Krabbe disease**. *ACS Catal* 2020, **10**:12091–12097.
Excellent example of the use of QM/MM metadynamics and MD to understand the CAZymes catalytic mechanism and deficiencies associated with specific mutations linked to rare diseases.

37. Foley BL, Tessier MB, Woods RJ: **Carbohydrate force fields**. *Wiley Interdiscip Rev Comput Mol Sci* 2012, **2**:652–697.

38. Fadda E, Woods RJ: **Molecular simulations of carbohydrates and protein–carbohydrate interactions: motivation, issues and prospects**. *Drug Discov Today* 2010, **15**:596–609.

39. Kirschner KN, Yongye AB, Tschampel SM, González-Outeiriño J, Daniels CR, Foley BL, Woods RJ: **GLYCAM06: a generalizable biomolecular force field. Carbohydrates**. *J Comput Chem* 2008, **29**:622–655.

40. Tessier MB, DeMarco ML, Yongye AB, Woods RJ: **Extension of the GLYCAM06 biomolecular force field to lipids, lipid bilayers and glycolipids**. *Mol Simulat* 2008, **34**:349–364.

41. Singh A, Tessier MB, Pederson K, Wang X, Venot AP, Boons G-J, Prestegard JH, Woods RJ: **Extension and validation of the GLYCAM force field parameters for modeling glycosaminoglycans**. *Can J Chem* 2016, **94**:927–935.

42. Mallajosyula SS, Jo S, Im W, MacKerell Jr AD: **Molecular dynamics simulations of glycoproteins using CHARMM**. *Methods Mol Biol* 2015, **1273**:407–429.

43. Guvench O, Mallajosyula SS, Raman EP, Hatcher E, Vanommeslaeghe K, Foster TJ, Jamison FW, MacKerell AD: **CHARMM additive all-atom force field for carbohydrate derivatives and its utility in polysaccharide and carbohydrate–protein modeling**. *J Chem Theor Comput* 2011, **7**:3162–3180.

44. Guvench O, Hatcher ER, Venable RM, Pastor RW, Mackerell AD: **CHARMM additive all-atom force field for glycosidic linkages between hexopyranoses**. *J Chem Theor Comput* 2009, **5**:2353–2370.

45. Mallajosyula SS, Guvench O, Hatcher E, Mackerell Jr AD: **CHARMM additive all-atom force field for phosphate and sulfate linked to carbohydrates**. *J Chem Theor Comput* 2012, **8**:759–776.

46. Raman EP, Guvench O, MacKerell Jr AD: **CHARMM additive all-atom force field for glycosidic linkages in carbohydrates involving furanoses**. *J Phys Chem B* 2010, **114**:12981–12994.

47. Schjoldager KT, Narimatsu Y, Joshi HJ, Clausen H: **Global view of human protein glycosylation pathways and functions**. *Nat Rev Mol Cell Biol* 2020, **21**:729–749.

48. Paschinger K, Wilson IBH: **Comparisons of N-glycans across invertebrate phyla**. *Parasitology* 2019, **146**:1733–1742.

49. Deshpande N, Wilkins MR, Packer N, Nevalainen H: **Protein glycosylation pathways in filamentous fungi**. *Glycobiology* 2008, **18**:626–637.

50. Rahman MU, Rehman AU, Liu H, Chen H-F: **Comparison and evaluation of force fields for intrinsically disordered proteins**. *J Chem Inf Model* 2020, **60**:4912–4923.

51. Robustelli P, Piana S, Shaw DE: **Developing a molecular dynamics force field for both folded and disordered protein states**. *Proc Natl Acad Sci U S A* 2018, **115**:E4758–E4766.

52. Weiß RG, Losfeld M-E, Aebi M, Riniker S: **N-glycosylation enhances conformational flexibility of protein disulfide isomerase revealed by microsecond molecular dynamics and markov state modeling**. *J Phys Chem B* 2021, **125**:9467–9479.

53. More AS, Toth 4th RT, Okbazghi SZ, Middaugh CR, Joshi SB, Tolbert TJ, Volkin DB, Weis DD: **Impact of glycosylation on the local backbone flexibility of well-defined IgG1-fc glycoforms using hydrogen exchange-mass spectrometry**. *J Pharmaceut Sci* 2018, **107**:2315–2324.

54. Johnson QR, Lindsay RJ, Raval SR, Dobbs JS, Nellas RB, Shen T: **Effects of branched O-glycosylation on a semiflexible peptide linker**. *J Phys Chem B* 2014, **118**:2050–2057.

55. Zerze GH, Mittal J: **Effect of O-linked glycosylation on the equilibrium structural ensemble of intrinsically disordered polypeptides**. *J Phys Chem B* 2015, **119**:15583–15592.

56. Plazinski W, Lonardi A, Hünenberger PH: **Revision of the GROMOS 56A6(CARBO) force field: improving the description of ring-conformational equilibria in hexopyranose-based carbohydrates chains**. *J Comput Chem* 2016, **37**:354–365.

57. Nester K, Gaweda K, Plazinski W: **A GROMOS force field for furanose-based carbohydrates**. *J Chem Theor Comput* 2019, **15**:1168–1186.

58. Lins RD, Hünenberger PH: **A new GROMOS force field for hexopyranose-based carbohydrates**. *J Comput Chem* 2005, **26**:1400–1412.

59. Pol-Fachin L, Rusu VH, Verli H, Lins RD: **GROMOS 53A6GLYC, an improved GROMOS force field for hexopyranose-based carbohydrates**. *J Chem Theor Comput* 2012, **8**:4681–4690.

60. Kony D, Damm W, Stoll S, Van Gunsteren WF: **An improved OPLS-AA force field for carbohydrates**. *J Comput Chem* 2002, **23**:1416–1429.

61. Jamali SH, van Westen T, Moultos OA, Vlugt TJH: **Optimizing nonbonded interactions of the OPLS force field for aqueous solutions of carbohydrates: how to capture both thermodynamics and dynamics**. *J Chem Theor Comput* 2018, **14**: 6690–6700.

62. Vanommeslaeghe K, MacKerell Jr AD: **CHARMM additive and polarizable force fields for biophysics and computer-aided drug design**. *Biochim Biophys Acta* 2015, **1850**:861–871.

63. Nerenberg PS, Head-Gordon T: **New developments in force fields for biomolecular simulations**. *Curr Opin Struct Biol* 2018, **49**:129–138.

64. Huang J, MacKerell Jr AD: **Force field development and simulations of intrinsically disordered proteins**. *Curr Opin Struct Biol* 2018, **48**:40–48.

65. Mu J, Liu H, Zhang J, Luo R, Chen H-F: **Recent force field strategies for intrinsically disordered proteins**. *J Chem Inf Model* 2021, **61**:1037–1047.

66. Qiu Y, Shan W, Zhang H: **Force field benchmark of amino acids. 3. Hydration with scaled Lennard-Jones interactions**. *J Chem Inf Model* 2021, **61**:3571–3582.

67. Zhang H, Yin C, Jiang Y, van der Spoel D: **Force field benchmark of amino acids: I. Hydration and diffusion in different water models**. *J Chem Inf Model* 2018, **58**:1037–1052.

68. ** Lemkul JA, Huang J, Roux B, MacKerell Jr AD: **An empirical polarizable force field based on the classical Drude oscillator model: development history and recent applications**. *Chem Rev* 2016, **116**:4983–5013.
Excellent and comprehensive review of the implementation and effects of the introduction of polarization to MD simulations based on empirical force field through the Drude oscillator model.

69. Bashardanesh Z, van der Spoel D: **Impact of dispersion coefficient on simulations of proteins and organic liquids**. *J Phys Chem B* 2018, **122**:8018–8027.

70. * Walters ET, Mohebifar M, Johnson ER, Rowley CN: **Evaluating the london dispersion coefficients of protein force fields using the exchange-hole dipole moment model**. *J Phys Chem B* 2018, **122**:6690–6701.
Empirical origin of the successful representation of dispersion forces in empirical force fields through the overestimation of the C6 dispersion coefficients in the Lennard–Jones potential to account for the neglected higher order terms.

71. Kadaoluwa Pathirannahalage SP, Meftahi N, Elbourne A, Weiss ACG, McConville CF, Padua A, Winkler DA, Costa Gomes M, Greaves TL, Le TC, *et al.*: **Systematic comparison of the structural and dynamic properties of commonly used water models for molecular dynamics simulations**. *J Chem Inf Model* 2021, **61**:4521–4536.

72. Lazar RD, Akher FB, Ravenscroft N, Kuttel MM: **Carbohydrate force fields: the role of small partial atomic charges in preventing conformational collapse**. *J Chem Theor Comput* 2022, **18**:1156–1172.

73. ** Lay WK, Miller MS, Elcock AH: **Optimizing solute–solute interactions in the GLYCAM06 and CHARMM36 carbohydrate force fields using osmotic pressure measurements**. *J Chem Theor Comput* 2016, **12**:1401–1407.
Shortcomings of the CHARMM36 and GLYCAM06 parameter sets for the simulation of glucose and sucrose solutions and recovery of experimental osmotic pressure measurements by scaling Lennard–Jones parameters.

74. Sauter J, Grafmüller A: **Solution properties of hemicellulose polysaccharides with four common carbohydrate force fields**. *J Chem Theor Comput* 2015, **11**:1765–1774.

75. Hadden JA, French AD, Woods RJ: **Unraveling cellulose microfibrils: a twisted tale**. *Biopolymers* 2013, **99**:746–756.

76. Mahoney MW, Jorgensen WL: **A five-site model for liquid water and the reproduction of the density anomaly by rigid, nonpolarizable potential functions**. *J Chem Phys* 2000, **112**: 8910–8922.

77. Mahoney MW, Jorgensen WL: **Diffusion constant of the TIP5P model of liquid water**. *J Chem Phys* 2001, **114**:363–366.

78. Fadda E, Woods RJ: **On the role of water models in quantifying the binding free energy of highly conserved water molecules in proteins: the case of concanavalin A**. *J Chem Theor Comput* 2011, **7**:3391–3398.

79. Best RB, Mittal J: **Protein simulations with an optimized water model: cooperative helix formation and temperature-induced unfolded state collapse**. *J Phys Chem B* 2010, **114**: 14916–14923.

80. * Alibay I, Burusco KK, Bruce NJ, Bryce RA: **Identification of rare Lewis oligosaccharide conformers in aqueous solution using enhanced sampling molecular dynamics**. *J Phys Chem B* 2018, **122**:2462–2474.
Direct comparison of conventional and enhanced sampling MD schemes used to explore the conformational equilibrium and associated energy profiles of the Lewis X epitope, with implications on its recognition.

81. * Turupcu A, Oostenbrink C: **Modeling of oligosaccharides within glycoproteins from free-energy landscapes**. *J Chem Inf Model* 2017, **57**:2222–2236.
A library of conformational free–energy profiles of glycosidic linkages is used in this work to approach the construction of N- and O-glycan structures in a bottom-up approach, extended to trisaccharides and tetrasaccharides

82. Nishima W, Miyashita N, Yamaguchi Y, Sugita Y, Re S: **Effect of bisecting GlcNAc and core fucosylation on conformational properties of biantennary complex-type N-glycans in solution**. *J Phys Chem B* 2012, **116**:8504–8512.

83. Nakano M, Mishra SK, Tokoro Y, Sato K, Nakajima K, Yamaguchi Y, Taniguchi N, Kizuka Y: **Bisecting GlcNAc is a general suppressor of terminal modification of N-glycan**. *Mol Cell Proteomics* 2019, **18**:2044–2057.

84. ** Topin J, Lelimousin M, Arnaud J, Audfray A, Pérez S, Varrot A, Imberty A: **The hidden conformation of Lewis x, a human histo-blood group Antigen, is a determinant for recognition by pathogen lectins**. *ACS Chem Biol* 2016, **11**: 2011–2020.
Recognition of the rare 'open' conformation of the Lewis X trisaccharide by the *Ralstonia solanacearum* lectin through X-ray crystallography and MD simulations underscores the importance of extensive sampling to study glycan-lectin binding.

85. Mathew C, Gregor Weiß R, Giese C, Lin C-W, Losfeld M-E, Glockshuber R, Riniker S, Aebi M: **Glycan–protein interactions determine kinetics of N -glycan remodeling**. *RSC Chemical Biology* 2021, https://doi.org/10.1039/D1CB00019E.

86. Harbison A, Fadda E: **An atomistic perspective on antibody-dependent cellular cytotoxicity quenching by core-fucosylation of IgG1 Fc N-glycans from enhanced sampling molecular dynamics**. *Glycobiology* 2020, **30**:407–414.

87. Göritzer K, Turupcu A, Maresch D, Novak J, Altmann F, Oostenbrink C, Obinger C, Strasser R: **Distinct Fcα receptor N-glycans modulate the binding affinity to immunoglobulin A (IgA) antibodies**. *J Biol Chem* 2019, **294**:13995–14008.

88. Aytenfisu AH, Deredge D, Klontz EH, Du J, Sundberg EJ, MacKerell Jr AD: **Insights into substrate recognition and specificity for IgG by Endoglycosidase S2**. *PLoS Comput Biol* 2021, **17**, e1009103.

89. Fadda E: **Understanding the structure and function of viral glycosylation by molecular simulations: state-of-the-art and recent case studies**. *Reference Module in Chemistry, Molecular Sciences and Chemical Engineering* 2020, https://doi.org/10.1016/B978-0-12-819475-1.00056-0.

90. Yang M, Huang J, Simon R, Wang L-X, MacKerell AD: **Conformational heterogeneity of the HIV envelope glycan shield**. *Sci Rep* 2017, **7**.

91. ** Casalino L, Gaieb Z, Goldsmith JA, Hjorth CK, Dommer AC, Harbison AM, Fogarty CA, Barros EP, Taylor BC, McLellan JS, *et al.*: **Beyond shielding: the roles of glycans in the SARS-CoV-2 spike protein**. *ACS Cent Sci* 2020, **6**:1722–1734.
Multimicrosecond MD simulations in combination with biolayer interferometry experiments show for the first time in a viral protein the key

role of the glycan shield, and more specifically of the N-glycans at specific positions, in the structure and activity of the S glycoprotein.

92. ** Sztain T, Ahn S-H, Bogetti AT, Casalino L, Goldsmith JA, Seitz E, McCool RS, Kearns FL, Acosta-Reyes F, Maji S, *et al.*: **A glycan gate controls opening of the SARS-CoV-2 spike protein**. *Nat Chem* 2021, https://doi.org/10.1038/s41557-021-00758-3.
Enhanced sampling in combination with cryo-EM and biolayer interferometry data shows the critical role of the N-glycan at N343 in gating the opening and closing of the S RBD.

93. ** Turoňová B, Sikora M, Schürmann C, Hagen WJH, Welsch S, Blanc FEC, von Bülow S, Gecht M, Bagola K, Hörner C, *et al.*: **In situ structural analysis of SARS-CoV-2 spike reveals flexibility mediated by three hinges**. *Science* 2020, **370**:203–208.
Multimicrosecond MD simulations of a cluster of S glycoproteins on the surface of the virus show the flexibility of the molecular architecture, providing an atomistic understanding of the cryo-ET images.

94. Sikora M, von Bülow S, Blanc FEC, Gecht M, Covino R, Hummer G: **Computational epitope map of SARS-CoV-2 spike protein**. *PLoS Comput Biol* 2021, **17**, e1008790.

95. Zhao P, Praissman JL, Grant OC, Cai Y, Xiao T, Rosenbalm KE, Aoki K, Kellman BP, Bridger R, Barouch DH, *et al.*: **Virus-receptor interactions of glycosylated SARS-CoV-2 spike and human ACE2 receptor**. *Cell Host Microbe* 2020, **28**:586–601. e6.

96. Brotzakis ZF, Löhr T, Vendruscolo M: **Determination of intermediate state structures in the opening pathway of SARS-CoV-2 spike using cryo-electron microscopy**. *Chem Sci* 2021, **12**:9168–9175.

97. Dommer A, Casalino L, Kearns F, Rosenfeld M, Wauer N, Ahn S-H, Russo J, Oliveira S, Morris C, Bogetti A, *et al.*: *#COVIDisAirborne: AI-enabled multiscale computational microscopy of delta SARS-CoV-2 in a respiratory aerosol*. bioRxiv; 2021, https://doi.org/10.1101/2021.11.12.468428.

98. * Pang YT, Acharya A, Lynch DL, Pavlova A, Gumbart JC: *SARS-CoV-2 spike opening dynamics and energetics reveal the individual roles of glycans and their collective impact*. bioRxiv; 2021, https://doi.org/10.1101/2021.08.12.456168.
MD simulations and 2D-replica exchange umbrella sampling calculations are used in this work to investigate the opening energetics and conformational equilibrium of the SARS-CoV-2 RBD in the presence and absence of the glycan shield.

99. Grant OC, Montgomery D, Ito K, Woods RJ: **Analysis of the SARS-CoV-2 spike protein glycan shield reveals implications for immune recognition**. *Sci Rep* 2020, **10**:14991.

100. Gawish R, Starkl P, Pimenov L, Hladik A, Lakovits K, Oberndorfer F, Cronin SJ, Ohradanova-Repic A, Wirnsberger G, Agerer B, *et al.*: **ACE2 is the critical in vivo receptor for SARS-CoV-2 in a novel COVID-19 mouse model with TNF- and IFNγ-driven immunopathology**. *Elife* 2022, **11**, e74623.

101. Hoffmann D, Mereiter S, Jin Oh Y, Monteil V, Elder E, Zhu R, Canena D, Hain L, Laurent E, Grünwald-Gruber C, *et al.*: **Identification of lectin receptors for conserved SARS-CoV-2 glycosylation sites**. *EMBO J* 2021, **40**, e108375.

102. Capraz T, Kienzl NF, Laurent E, Perthold JW, Föderl-Höbenreich E, Grünwald-Gruber C, Maresch D, Monteil V, Niederhöfer J, Wirnsberger G, *et al.*: **Structure-guided glyco-engineering of ACE2 for improved potency as soluble SARS-CoV-2 decoy receptor**. *Elife* 2021, **10**, e73641.

103. Thomson EC, Rosen LE, Shepherd JG, Spreafico R, da Silva Filipe A, Wojcechowskyj JA, Davis C, Piccoli L, Pascall DJ, Dillen J, *et al.*: **Circulating SARS-CoV-2 spike N439K variants maintain fitness while evading antibody-mediated immunity**. *Cell* 2021, **184**:1171–1187. e20.

104. * Zimmerman MI, Porter JR, Ward MD, Singh S, Vithani N, Meller A, Mallimadugula UL, Kuhn CE, Borowsky JH, Wiewiora RP, *et al.*: **SARS-CoV-2 simulations go exascale to predict dramatic spike opening and cryptic pockets across the proteome**. *Nat Chem* 2021, **13**:651–659.
MD simulations break the exascale barrier for the first time in history with the @FoldingatHome distributed computing platform for the simulation of the SARS-CoV-2 proteome.

105. * Paiardi G, Richter S, Oreste P, Urbinati C, Rusnati M, Wade RC: **The binding of heparin to spike glycoprotein inhibits SARS-CoV-2 infection by three mechanisms**. *J Biol Chem* 2021, **298**:101507.
Molecular docking and MD simulations of the interaction between SARS-CoV-2 S and heparin, supported by experimental assays, provide important mechanistic insight into the inhibition mechanism of viral infection by heparin.

106. * Schuurs ZP, Hammond E, Elli S, Rudd TR, Mycroft-West CJ, Lima MA, Skidmore MA, Karlsson R, Chen Y-H, Bagdonaite I, *et al.*: **Evidence of a putative glycosaminoglycan binding site on the glycosylated SARS-CoV-2 spike protein N-terminal domain**. *Comput Struct Biotechnol J* 2021, **19**:2806–2818.
Molecular docking and MD simulations are used here to provide insight into the binding of heparin and heparan sulfate 12-mers to the SARS-CoV-2 S, identifying a potential binding site on the NTD.

107. Kim SY, Jin W, Sood A, Montgomery DW, Grant OC, Fuster MM, Fu L, Dordick JS, Woods RJ, Zhang F, *et al.*: **Characterization of heparin and severe acute respiratory syndrome-related coronavirus 2 (SARS-CoV-2) spike glycoprotein binding interactions**. *Antivir Res* 2020, **181**:104873.

108. Pedebos C, Khalid S: **Simulations of the spike: molecular dynamics and SARS-CoV-2**. *Nat Rev Microbiol* 2022, https://doi.org/10.1038/s41579-022-00699-9.

109. Arantes PR, Saha A, Palermo G: **Fighting COVID-19 using molecular dynamics simulations**. *ACS Cent Sci* 2020, **6**:1654–1656.

110. ** Harbison AM, Fogarty CA, Phung TK, Satheesan A, Schulz BL, Fadda E: **Fine-tuning the spike: role of the nature and topology of the glycan shield in the structure and dynamics of the SARS-CoV-2 S**. *Chem Sci* 2022, **13**:386–395.
Multiple microsecond MD simulations show that the structure of N-glycans at positions determined to be critical for function affects the stability and dynamics of the open RBD. Also, changes in the topology of the glycan shield along the phylogeny promote RBD opening and optimize activity.

111. ** Kim SH, Kearns FL, Rosenfeld MA, Casalino L, Papanikolas MJ, Simmerling C, Amaro RE, Freeman R: **GlycoGrip: cell surface-inspired universal sensor for betacoronaviruses**. *ACS Cent Sci* 2022, **8**:22–42.
Molecular docking, in combination with MD simulations, support the design of a betacoronavirus diagnostic platform based on the S affinity for highly sulfated glycosaminoglycans (GAGs).

112. Fallon L, Belfon KAA, Raguette L, Wang Y, Stepanenko D, Cuomo A, Guerra J, Budhan S, Varghese S, Corbo CP, *et al.*: **Free energy landscapes from SARS-CoV-2 spike glycoprotein simulations suggest that RBD opening can Be modulated via interactions in an allosteric pocket**. *J Am Chem Soc* 2021, **143**:11349–11360.

113. Kang L, He G, Sharp AK, Wang X, Brown AM, Michalak P, Weger-Lucarelli J: *A selective sweep in the Spike gene has driven SARS-CoV-2 human adaptation*. bioRxiv; 2021, https://doi.org/10.1101/2021.02.13.431090.

114. Zhang S, Liang Q, He X, Zhao C, Ren W, Yang Z, Wang Z, Ding Q, Deng H, Wang T, *et al.*: **Loss of Spike N370 glycosylation as an important evolutionary event for the enhanced infectivity of SARS-CoV-2**. *Cell Res* 2022, https://doi.org/10.1038/s41422-021-00600-y.

115. Aytenfisu AH, Yang M, MacKerell Jr AD: **CHARMM Drude polarizable force field for glycosidic linkages involving pyranoses and furanoses**. *J Chem Theor Comput* 2018, **14**:3132–3143.

116. Pandey P, Aytenfisu AH, MacKerell Jr AD, Mallajosyula SS: **Drude polarizable force field parametrization of carboxylate and N-acetyl amine carbohydrate derivatives**. *J Chem Theor Comput* 2019, **15**:4982–5000.

117. Pandey P, Mallajosyula SS: **Influence of polarization on carbohydrate hydration: a comparative study using additive and polarizable force fields**. *J Phys Chem B* 2016, **120**:6621–6633.

118. Jana M, MacKerell AD: **CHARMM Drude polarizable force field for aldopentofuranoses and methyl-aldopentofuranosides**. *J Phys Chem B* 2015, **119**:7846–7859.

119. Jiang W, Hardy DJ, Phillips JC, Mackerell Jr AD, Schulten K, Roux B: **High-performance scalable molecular dynamics**

simulations of a polarizable force field based on classical Drude oscillators in NAMD. *J Phys Chem Lett* 2011, **2**:87–92.

120. Unke OT, Chmiela S, Sauceda HE, Gastegger M, Poltavsky I, Schütt KT, Tkatchenko A, Müller K-R: **Machine learning force fields**. *Chem Rev* 2021, **121**:10142–10186.

121. Smith JS, Isayev O, Roitberg AE: **ANI-1: an extensible neural network potential with DFT accuracy at force field computational cost**. *Chem Sci* 2017, **8**:3192–3203.

122. Yao K, Herr JE, Toth DW, Mckintyre R, Parkhill J: **The TensorMol-0.1 model chemistry: a neural network augmented with long-range physics**. *Chem Sci* 2018, **9**:2261–2269.

123. Thölke P, De Fabritiis G: *TorchMD-NET: equivariant transformers for neural network based molecular potentials.* arXiv [csLG]; 2022. 2202.02541.

124. Outeiral C, Strahm M, Shi J, Morris GM, Benjamin SC, Deane CM: **The prospects of quantum computing in computational molecular biology**. *Wiley Interdiscip Rev Comput Mol Sci* 2021, **11**:e1481.

125. Grimsley HR, Economou SE, Barnes E, Mayhall NJ: **An adaptive variational algorithm for exact molecular simulations on a quantum computer**. *Nat Commun* 2019, **10**:3007.

126. Ollitrault PJ, Miessen A, Tavernelli I: **Molecular quantum dynamics: a quantum computing perspective**. *Acc Chem Res* 2021, **54**:4229–4238.

127. Cao Y, Romero J, Olson JP, Degroote M, Johnson PD, Kieferová M, Kivlichan ID, Menke T, Peropadre B, Sawaya NPD, *et al.*: **Quantum chemistry in the age of quantum computing**. *Chem Rev* 2019, **119**:10856–10915.